Moisture transport in coated wood

P.A. van Meel[a], S.J.F. Erich[a,b,*], H.P. Huinink[a], K. Kopinga[a], J. de Jong[b], O.C.G. Adan[a,b]

[a] Department of Applied Physics, Eindhoven University of Technology, P.O. Box 513, 5600 MB Eindhoven, The Netherlands
[b] TNO, P.O. Box 49, 2600 AA Delft, The Netherlands

ARTICLE INFO

ABSTRACT

Moisture accumulation inside wood causes favorable conditions for decay. Application of a coating alters the moisture sorption of wood and prevents accumulation of moisture. This paper presents the results of a nuclear magnetic resonance (NMR) study on the influence of a coating on the moisture absorption of wood.

NMR allows to determine both local wood moisture content and rate of water absorption during water absorption and desorption of coated and uncoated wood. In contrast to weighing, both quantities are measured dynamically and non destructively with high spatial and temporal resolution in relatively short experiments. In addition, NMR relaxometry distinguishes between moisture in lumina and moisture in cell walls, which allows to accurately characterize sorption processes in wood. In the present study, samples with a diameter of 20 mm and a height of 10 mm, are studied in a 4.7 T NMR scanner with a spatial resolution of $33 \pm 3\,\mu m$.

Several commonly used wood–coating combinations are studied. Water is placed on the tangential side of samples equilibrated at 22% relative humidity while the wood moisture content (MC) is monitored for 24 h. This research shows that the sorption behavior of coated wood depends on the specific combination of wood and coating. Additionally, the amount of water that is absorbed in a coating may have a strong influence on the moisture content of the coated wood.

We found that the water absorption of a hardwood dark red meranti sample is diffusion dominated. Application of a waterborne acrylic coating has no influence on this absorption process, which is attributed to the large water uptake of the coating. A solvent borne alkyd coating that absorbs very little water is found to strongly reduce the water uptake of the meranti studied. The waterborne coating reduces the water uptake of pine by preventing capillary water uptake of rays present in this softwood. The solvent borne alkyd coating further reduces uptake. Uncoated spruce also absorbs water by capillary suction. On this wood, the acrylic coating strongly reduces the water uptake; comparable to alkyd coated spruce. This is a result of the pits of spruce which became aspirated during drying. Application of a coating might fixate the aspirated pits, resulting in a structure with low permeability.

1. Introduction

1.1. Wood and coatings

A major disadvantage of wood is its susceptibility to degradation due to environmental influences like temperature, radiation or damage from biological, mechanical or chemical attacks. Furthermore, all wood is sensitive to moisture, which not only causes swelling and shrinkage, but also favorable conditions for biological decay like wood rot.

Application of a coating provides protection of wood against weathering, besides adding the desired aesthetical properties, e.g. color and gloss. A coating decreases the weathering of a wood surface as a coatings' barrier function against water transport reduces the rate of water uptake. It also reduces the drying rate of wood. The interest in coating permeability has gained interest with the introduction of waterborne paints, which generally exhibit a higher moisture affinity than solvent borne coatings. In addition, the concern regarding the effect of chemicals on health and environment has increased considerably in the past twenty years, leading to stricter legislation concerning the emission and usage of volatile organic components (VOCs) [1–4]. This drives coating manufacturers to reformulate and subsequently produce more and more waterborne coatings. Nowadays, more than 95% of exterior wood

* Corresponding author at: Eindhoven University of Technology, Applied Physics, Nl b 1.02, Den Dolech 2, P.O. Box 513, 5600 MB Eindhoven, The Netherlands.
Tel.: +31 40 247 3830; fax: +31 40 243 2598.
E-mail address: s.j.f.erich@tue.nl (S.J.F. Erich).
URL: http://www.phys.tue.nl/TPM (S.J.F. Erich).

coatings are applied in liquid form with either an organic solvent or water as the carrier for the other coating ingredients.

1.2. Measuring wood moisture content

The influence of coating systems on the moisture content of wood has been recognized for a long time. To study this influence, several approaches have been used. These include permeability measurements of free coating films or coated wood samples, moisture content monitoring in practice on panels or full scale wooden constructions [5]. Much effort is put into the understanding and modeling of drying processes of uncoated wood to shorten industrial kiln drying times using techniques such as weighing and X-ray tomography [6–9]. Weighing studies have shown that water absorption – a combined process of diffusion and capillary water uptake – is strongly influenced by a coating [10,11]. However, weighing yields no or low spatial resolution and is time consuming. Currently, the performance of a coating is tested according to norms, such as EN927. However, these tests only assess the performance of a coating. None of the common techniques reveal the exact moisture behavior and underlying transport mechanisms and thus do not lead to fundamental understanding.

To understand the moisture transport in coated wood, it is necessary to measure the moisture content dynamically and quantitatively. It has been shown that nuclear magnetic resonance (NMR) is a powerful technique to do so [12–15]. NMR allows to measure the wood moisture content non-invasively with high spatial and temporal resolution. In addition, NMR measurements allow to discriminate water in cell walls (bound water) from water in lumina and vessels (free water) [16–21].

The goal of the research presented in this paper was to study the influence of wood structure and coating type on the water uptake of coated wood. Four types of wood were studied by NMR: one hardwood (dark red meranti), two softwoods (pine and spruce) and acetylated pine. Meranti and spruce were chosen because of their frequent application in building and their difference in water uptake process. Pine and acetylated pine were compared to study the effect of acetylation. Three commercially available coating types were used: a non film-forming waterborne alkyd stain, a waterborne acrylic and a solvent born alkyd.

Section 2 reviews the structure of wood and the behavior of moisture in wood. In Section 3 the materials and methods are explained: details of the used wood and coating types, samples, and sample holder, as well as the NMR principles, settings and calibration. Section 4 gives the results of the measurements on meranti, Section 5 those of pine and Section 6 those of spruce. Finally, Section 7 summarizes our findings and conclusions.

2. Wood

2.1. Structure of wood

Wood is build up of cells [22]. Although wood cells are complex structures, for our moisture considerations the distinction between voids (such as lumina, vessels and rays) and cell walls suffices. Wood is a porous material and moisture in wood is present in two basic forms. The first is bound water within the cell wall, which is considered bound on and between cellulose fibers in the cell wall. The second is unbound water in the voids of the wood such as lumina and vessels. The amount of water in wood is expressed as a moisture content (MC) Θ, which is defined as the ratio of the mass of water in the wood and the oven dry mass of wood, expressed as a percentage:

$$\Theta = \frac{w_m - w_0}{w_0} \times 100. \tag{1}$$

where w_m is the mass of the wet wood. The oven dry mass w_0 is defined as the constant mass obtained after wood has dried in an oven maintained at $102 \pm 3\,°C$. Cell walls exchange moisture with air surrounding the wood and an equilibrium is established between the bound water and the water vapor in the surrounding air. The RH is defined as:

$$RH = \frac{p}{p_0} \times 100, \tag{2}$$

where p is the partial vapor pressure in the air and p_0 is the saturated vapor pressure at the given temperature of the air.

2.1.1. Fiber saturation point

The so-called equilibrium moisture content (EMC) increases with the RH until the cell walls become saturated when the RH approaches 100%. This point is called the fiber saturation point (FSP) which is reached in practice at approximately 98% RH [22]. For most wood types, the FSP corresponds to a MC of approximately 30%. Above the FSP, additional water is present in the unbound form in the lumina or voids of the wood. The porosity of the wood limits the maximum amount of unbound water.

2.1.2. Moisture sorption by wood

Fig. 1 shows the various stages of water sorption in wood. Fig. 1(a) shows two adjacent cells with their cell walls and lumina in case the wood is fully saturated: the cell walls and lumina are filled with water. The first stage of desorption is when the lumina are drying although the cell walls are still fully saturated, as shown in Fig. 1(b). Unbound water is not a source for swelling or shrinkage since it is held only by relatively weak capillary forces. In Fig. 1(c) the lumina have dried completely, but the cell walls are still saturated; this is the fiber saturation point. With progressed drying, the bound water starts to desorb from the cell walls and is transported to the surface via vapor diffusion through the lumina and vessels, Fig. 1(d). Since shrinkage and swelling are attributed to bound water, this process causes radial and tangential shrinkage. Any change in longitudinal direction is minor. Fig. 1(e) shows the fully dehydrated cells. The process is largely reversible, although usually hysteresis occurs.

2.1.3. Moisture transport in wood

In all wood types, bound water is transported within a cell wall by diffusion. Moisture exchange between adjacent cell walls and/or with outside air takes place via vapor diffusion through lumina and via the pits that connect adjacent cells. Transport directly from cell wall to cell wall is negligible since the permeability of cell walls is very low [22].

Unbound moisture is transported differently in softwoods and hardwoods. Rays are a more important flow path in softwoods than in hardwoods. In pine, resin canals contribute significantly to the flow. In spruce, the radial permeability is low because the permeability and the volumetric fraction of the rays is low. Vessels are the most permeable axial flow path in hardwoods. The rays of hardwood generally contribute less to the overall flow than those of softwoods. For hardwoods there is little difference between radial and tangential permeability.

2.2. Acetylation

Chemical modification of the cell walls can increase the durability of fast growing and generally lower grade woods. One of the possible modifications is acetylation [23]. In the process of acetylation, acetyl groups form permanent covalent bonds with hydroxyl (OH) sites in wood cell walls. Acetylated wood provides an increase in dimensional stability under varying relative humidity because
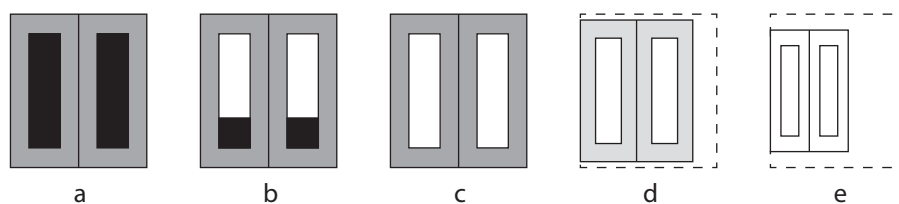
Fig. 1. Moisture in wood.

the acetyl groups occupy space in the cell wall, thereby decreasing the amount of water that can be absorbed. Consequently, the acetylated wood is in a permanently swollen condition. The extent of swelling depends on the level of modification.

3. Materials and methods

3.1. Wood and coating types

Four types of wood were studied: one type of hardwood, dark red meranti heartwood (Shorea Sapupira) and two types of softwood, pine (*Pinus radiata*) and spruce (Norway *Picea abies*), and acetylated pine. Three coating types were used which were sprayed in two or four layers: an open coating, being a waterborne non film-forming alkyd emulsion stain, a film-forming waterborne acrylic coating and a film-forming solvent borne alkyd coating, respectively. The non film-forming coating has viscosity of 300–400 mPa s, a glass transition temperature (T_g) of less than 0 °C, and a particle size less than 30 µm. The PVC of this coating is 15% and the solid content is 16% in volume. The acrylic coating has a viscosity of 1800 mPa s, the pigment particle size is less than 15 µm, and has a solid content of 40% in volume with a PVC of around 22%. This acrylic coating has a glass transition temperature of less than 0 °C. The alkyd has a viscosity of 1200 mPa s, and pigment particles size is smaller than 10 µm, and has a solid content 66% in volume with a PVC of 15.7%. The T_g is not known for the alkyd coating. The wood types were studied uncoated and with a coating thickness of 100 and 200 µm for both the alkyd and acrylic coating, and applied masses of 50 and 150 g m^{-2} for the open coating. To study the influence of surface treatment, the wood surface was either planed of sanded before coating application. After application of the coating the samples were dried for at least 2 months before experiments started and the samples were equilibrated. The absorption was monitored by NMR for 24 h. In addition, for meranti, a coating thickness of 200 µm and a mass of 150 g m^{-2} were included to study the influence of coating thickness.

3.2. Samples and sample holder

Cylindrical samples were used with a diameter of 20 mm and a height of 10 mm, as shown schematically in Fig. 2. The coating is applied on the tangential plane for meranti and pine and on the radial plane for spruce. The samples were machined from coated wooden boards by milling at high spindle speeds. The sample holders were designed to seal the sides of the sample, only allowing moisture to enter or leave the wood through the coating. The
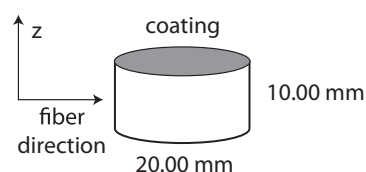

Fig. 2. Schematic representation of a sample.

sample holders were made of Teflon to prevent interference with the ^{1}H NMR signal.

3.3. Principles of NMR

Magnetic resonance imaging (MRI) is a well known NMR technique for making images of the human body. Its principle is based on the fact that magnetic nuclei located in a magnetic field have a specific resonance frequency, and can be excited by a radio frequency (RF) pulse. The resonance frequency f [Hz] depends linearly on the magnitude of the applied magnetic field $\vec{B}$ [T] according to $f = \gamma |\vec{B}|$, where γ [Hz/T] is the gyromagnetic ratio (for hydrogen nuclei, $\gamma = 42.58$ MHz/T). To obtain spatial information the resonance frequency is made to vary with position according to $f = \gamma(B_0 + zG_z)$, where $G_z = \partial B_z/\partial z$ [T/m] denotes an applied field gradient in the z-direction and B_0 the main magnetic field in the z-direction. The NMR signal (S) not only gives information on the density (concentration) of the magnetic nuclei (spins) ρ, in our case hydrogen nuclei, but also on the mobility of these nuclei. A cell wall restricts the mobility of the hydrogen atoms of water present within the cell wall. This is reflected in a decrease of the transverse relaxation time T_2 that describes the decay of the NMR signal. The relaxation time of free water is generally one or more orders of magnitude larger than that of bound water [16–21]. This allows to distinguish water in the cell walls (bound water) from water in lumina and vessels (free water).

3.4. NMR settings

A main magnetic field of 4.7 T was used, resulting in a resonance frequency of approximately 200 MHz. Three pulse sequences where used. A Hahn Spin Echo (HSE) sequence [24], $90°_x - \tau - 180°_y - \tau - echo - \tau$ with $t_e = 2\tau$, was used to obtain one dimensional hydrogen density profiles. The signal intensity was calibrated allowing transformation to moisture content as explained in Section 3.5. Every point of a profile thus reflects the average MC of a round slice of the sample, perpendicular to the z-axis. A CarrPurcellMeiboomGill (CPMG) sequence recording 1000 echoes, $90°_x - \tau - [180°_y - \tau - echo - \tau]_n$, was used to measure the T_2-relaxation, yielding spatially resolved relaxation time distributions.

The parameters of the HSE and CPMG sequences are displayed in Table 1. The scanner uses a dynamic z-gradient with a maximum field strength of 752 mT/m. Δx_t is the theoretical resolution. For both the HSE and the CPMG sequence, the frequency encoding gradient is applied in the z-direction, i.e. parallel to B_0. x and y-gradients were used to align $\vec{G}$ exactly perpendicular to the sample surface to optimize the resolution. For the HSE measurements this

Table 1
Measurement parameters for the HSE and CPMG pulse sequences.

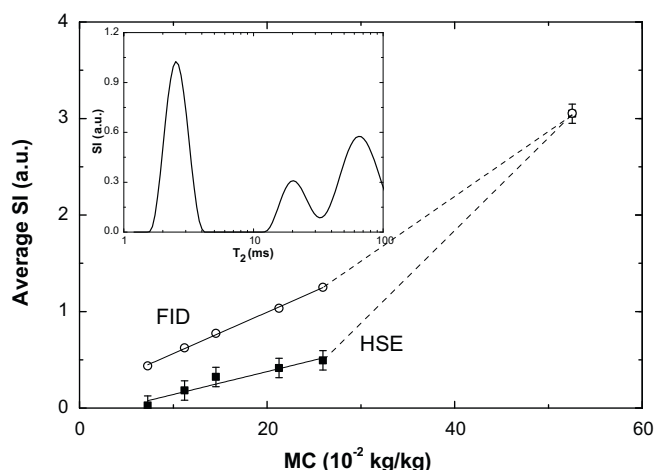|	t_e (ms)	G_z (mT/m)	Δx_t (µm)	N_{avg}	t_{acq} (min)
HSE	1.7	752	31	128	6.4
CPMG	1.2	300	78	128	8.8

Fig. 3. Average FID and HSE signal intensity of meranti equilibrated at 22%, 53%, 75%, 93% and 100% RH and at saturation. For MCs above the FSP, the SI is assumed to increase linearly with the MC. The inset shows the relaxation time distribution for a saturated sample.

Fig. 4. Moisture content profiles of the wetting of uncoated meranti; Δt = 139 min, t = 21 h.

resulted in a resolution of $33 \pm 3 \, \mu$m. N_{avg} is the number of signal averages and t_{acq} is the acquisition time for one profile. A long delay of 3 s and pulse durations of t_{90} = 65 and t_{180} = 120 μs were used in all measurements.

3.5. Measuring wood moisture content by NMR

The signal intensity (SI) of the HSE sequence was calibrated to obtain the wood moisture content. For this purpose, samples of all four wood types were equilibrated at 22%, 53%, 75%, 93% and 100% RH above saturated salt solutions. One sample of each type was fully saturated through immersion in water. The average SI, wet mass and oven dry mass of each sample were measured. The EMC of each sample is calculated from the masses and plotted against the corresponding average SI, shown for meranti in Fig. 3. The MC is given as a percentage of the oven dry weight, which corresponds to 10^{-2} kg/kg, see Eq. (1).

A change in slope of the HSE SI occurs at the FSP, due to a difference in relaxation time for bound and unbound water. The shortest relaxation time that can be measured equals the echo time of the CPMG sequence, t_e = 1200 μs. Note that the signal from solid wood decays within in tens of microseconds and is therefore not measured [16]. A relaxation time distribution measured on a fully saturated sample, see the inset of Fig. 3, shows peaks at low and at higher relaxation times. The first results from bound water. The latter results from unbound water. This is confirmed by a relaxation time distribution measured on a sample equilibrated at 100% RH – therefore containing bound water only – which showed a single peak at a relaxation time similar to the left peak in Fig. 3. Note that the intensity of a relaxation time contribution is indicated by the surface area of a peak, not by its height, and that the horizontal axis is logarithmic.

Because of the difference in relaxation times, the bound water signal has decayed more than the unbound water signal at the first moment of acquisition. By using a so-called free induction decay (FID) measurement the signal can already be measured 0.1 ms after excitation, compared to 1.7 ms for a HSE. As a consequence of this early signal acquisition the short relaxation times can be better observed, and consequently the change in slope at the FSP is significantly smaller for the FID SI plotted against MC as can be seen in Fig. 3.

Since the NMR SI is directly related to the hydrogen density, the SI is assumed to increase linearly with the MC for MCs above the
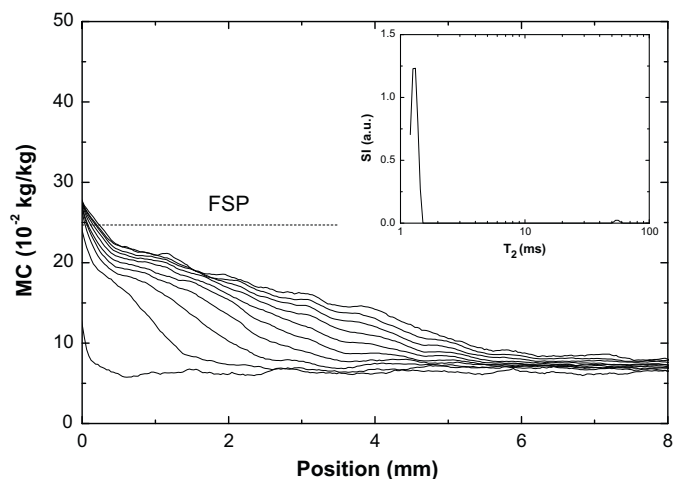
FSP. For each wood type, the SI is fitted with straight lines below and above the FSP. These fits are used to convert the HSE SI to MC. Note that this calibration is only valid if bound and free water are in equilibrium.

4. Absorption experiments on meranti

4.1. Moisture profiles during wetting

Moisture content profiles of the wetting of uncoated meranti are given in Fig. 4. The top of the sample is located at position x = 0. The time between each profile is given by Δt; the duration of the experiment by t. These profiles were obtained by interpolation over time and position of 68 profiles, measured every 21 min. All samples were equilibrated at 22% RH corresponding to an initial MC of about 7%. The error in the MC is approximately 1×10^{-2} kg/kg; the irregularities of the profiles are a result of wood inhomogeneities. The horizontal dashed line indicates the FSP as determined by the calibration, see Section 3.5.

The profiles in Fig. 4 show that the MC remains below the FSP. This is confirmed by the relaxation time distribution at the end of the experiment which is shown in the inset of Fig. 4. Only directly below the surface of the sample the MC exceeds the FSP, because of direct contact of lumina with water at the surface. The contribution at short relaxation times represents bound water.

Profiles were obtained similarly for coated meranti samples. Only minor water ingress is observed in case of alkyd coated meranti, indicating that the alkyd coating forms an effective barrier against moisture. Profiles of open coated meranti and of acrylic coated meranti display similar behavior as uncoated meranti. These similarities are confirmed by mass measurements. The relative mass change after 24 h of water uptake is displayed in Table 2.

Note that after 24 h the samples are not fully saturated. However, the profiles suggest that a steady-state is reached near the surface. This is confirmed by a six-day experiment, showing a stable MC close to the surface after one day. Firstly, this means that NMR offers a possibility to assess the absorption behavior of wood in considerably shorter experiments than other techniques [8–11]. Secondly, NMR allows to determine the MC of a sample in situ while water is still present on the sample.

4.2. Final water uptake

In order to compare the influence of the coatings on the water uptake of meranti, the average MC in a layer at the wood–coating

Table 2
Absolute and relative mass change of uncoated and coated meranti samples. The error in the absolute mass change is 0.1×10^2 g, that in the relative mass change is 0.1×10^{-2} g/g.

Coating	Applied mass (g m^{-2})	Thickness (μm)	Δm (10^2 g/m^2/24 h)	$\Delta m/m_0$ (10^{-2} g/g)
None			1.4	4.1
Open	50		1.3	3.8
	150		1.1	3.1
Alkyd		100	0.2	0.6
		200	0.2	0.3
Acrylic		100	1.4	4.0
		200	1.6	4.3

interface with a thickness of 1 mm is determined and plotted against time in Fig. 5. The figure confirms that the water uptake by alkyd coated meranti is low and that a thicker alkyd coating results in less uptake. For the other samples, the increase of the MC directly behind the surface slows down with time to reach a constant level after 24 h at a MC approximately equal to that of uncoated meranti. These results show that the open and acrylic coating have no influence on the amount of water uptake. The rate of water uptake is studied in the next section.

4.3. Rate of water uptake

The rate of water uptake is quantified by the diffusivity which can be determined directly from moisture profiles as explained below. Since the MC remains below the FSP, moisture transport takes place via vapor transport through the lumina, see Section 2.1.3. This diffusion process is described to a good approximation by a diffusion equation [25] that has a single solution if the diffusivity D is assumed constant:

$$MC(x, t) = EMC + (MC_s - EMC)\,\mathrm{erfc}\left(\frac{x}{\sqrt{4Dt}}\right), \qquad (3)$$

in which EMC is the MC of the wood sample prior to the experiment and MC_s is the MC at the surface of the wood when water is placed on the surface. This solution holds at $MC(0, t) = MC_0 = $ constant and as the incoming moisture has not reached the other boundary of the system at $x = L \rightarrow MC(L, t) = EMC$. The diffusivity D can be determined directly from moisture profiles, such as those given in Fig. 4, by applying the Boltzmann transformation and fitting the transformed profiles with Eq. (3). Fig. 6 shows the transformed moisture profiles of open coated meranti. All transformed profiles overlap, except for the first few since for these profiles the boundary condition $MC(0, t) = MC_0$ of the solution (Eq. (3)) is not met.

Fig. 6. Profiles of open coated meranti after Boltzmann transformation. The solid line is the fitted error function, Eq. (3), from which D is obtained.

The data is described very well by Eq. (3), implying that D can be treated as a constant in these experiments.

Profiles of 3 uncoated, 2 open coated and 6 acrylic (2 sanded and 4 planed) coated meranti samples were Boltzmann transformed and fitted. The resulting values for the diffusivity are given in Table 3. All values of D are equal within the error margin. In fact, the values correspond to the transverse (tangential and radial) diffusion coefficient of meranti of approximately 1×10^{-10} m^2 s^{-1} [22]. This means that the open and acrylic coating have no influence on the rate of water uptake of meranti.

4.4. Water uptake of the coatings

The open and acrylic coating have been found to have no influence on the rate and amount of water uptake of meranti over a period of 24 h. In order to explain this, the water uptake of the coating itself is studied. The resolution of 33 ± 3 μm allows to discriminate the alkyd and acrylic coating from wood. The open coating does not form a film, making it indistinguishable from the wood surface. Two to five NMR slices, depending on the coating thickness, were measured inside the alkyd and acrylic coating. The average SI of these slices is plotted against time in Fig. 7.

Alkyd coatings of both 100 and 200 μm thick apparently absorb hardly any water. This could explain why the alkyd coating forms
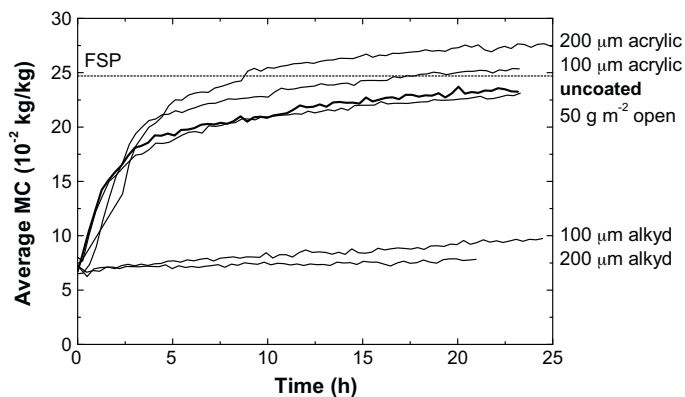

Fig. 5. Average MC of a 1 mm thick slice of meranti directly behind the coating–meranti interface, plotted against time. Coating thicknesses of 100 and 200 μm for both alkyd and acrylic coatings and applied mass of 50 g m^{-2} for the open coating are shown. The horizontal dashed line indicates the FSP. The bold curve represents the average MC of a similar slice of uncoated meranti.
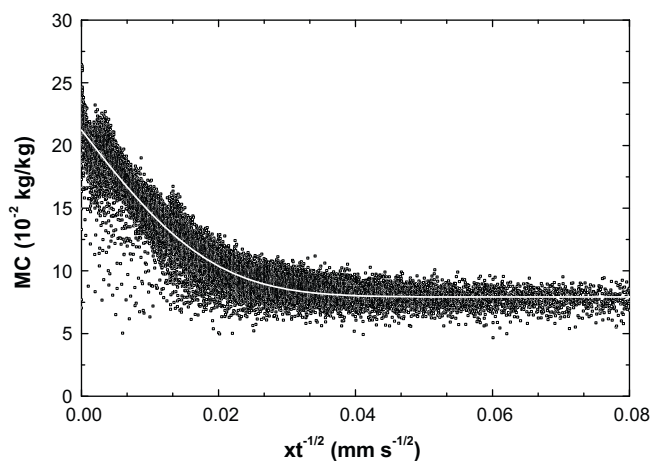
Table 3
Diffusion constant for coated and uncoated meranti as found from the Boltzmann transformed profiles. The error in D is 3.0×10^{-11} m^2 s^{-1}.

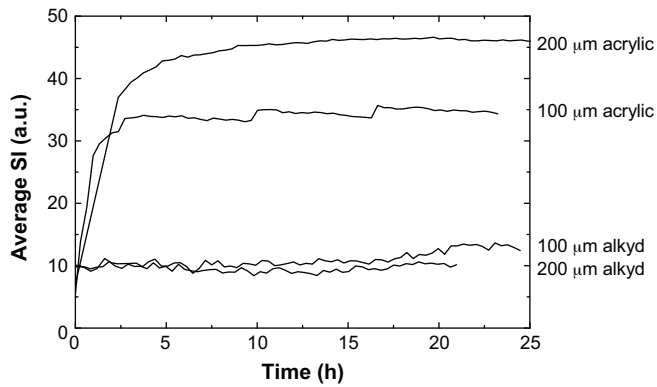| Coating	Mass (g m^{-2})	Thickness (μm)	D (10^{-11} m^2 s^{-1})
None			8.3
Open	50		11
	150		8.3
Acrylic		100	9.5
		200	8.4

Fig. 7. Average SI measured in the coating for coating a thickness of 100 and 200 μm.

an effective barrier against moisture. Opposite to this, the acrylic coating absorbs relatively large amounts of water. Since the values for the effective diffusivity of acrylic coated meranti, presented in Table 3, are all comparable to that of uncoated meranti, the acrylic coating does not influence the water uptake. As such, the acrylic coating does not seem to form an effective barrier since the absorption is fully limited by the wood. In addition, a small microscope study showed that the coating surface of arylic coated meranti was comparable that of alkyd coated meranti, both in thickness and unevenness. Thus coating defects were disregarded as an explanation. The fact that the coating itself takes up a relatively large amount of water does not necessarily mean that this explains the high water uptake. In fact, it is known that uptake and permeability of a coating can be quite different [26].

5. Absorption experiments on (acetylated) pine

5.1. Uncoated pine

Profiles of the water uptake of uncoated pine obtained by NMR are given in Fig. 8. The homogeneously increasing profiles indicate capillary water uptake immediately from the beginning of the experiment. As opposed to meranti, pine contains relatively large and highly permeable rays. These run in the radial direction, which is parallel to the z-axis as shown in Fig. 2. The rays quickly absorb water by capillary suction. A relaxation time distribution determined after 15 min of water uptake confirms this (Fig. 9). This already shows both bound and unbound contributions. The
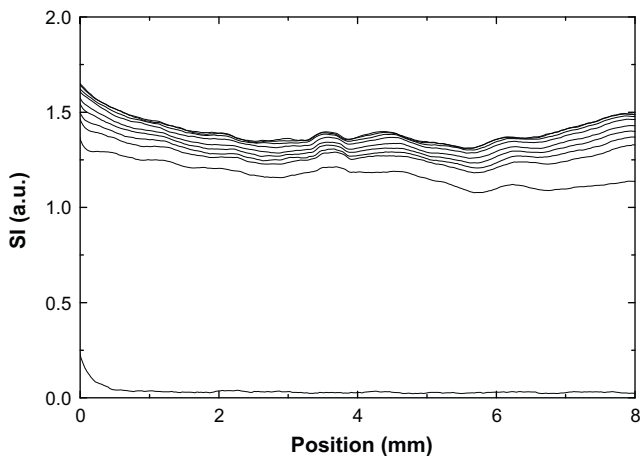

Fig. 8. Moisture content profiles of the wetting of uncoated pine; $\Delta t = 143$ min, $t = 21$ h. Note that the vertical axis shows signal intensity, as the calibration cannot be used, because of fast capillary water uptake by rays at the beginning of the experiment.
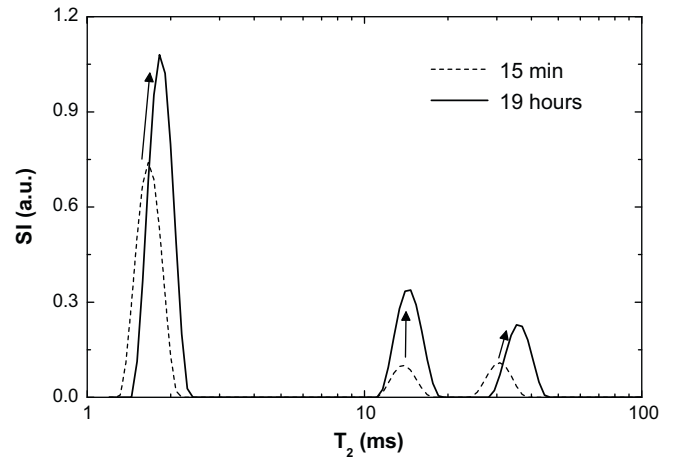

Fig. 9. Relaxation time distributions for uncoated pine after 15 min of water uptake, shown by the dashed curve and after equilibrium has been reached, shown by the solid curve.

relaxation time distribution obtained after 19 h shows that both the bound and unbound contributions have increased. This means that the rays, and possibly also the lumina, contain water before the cell walls are saturated. Bound and unbound water are not in equilibrium and, consequently, the signal calibration cannot be applied. However, the calibration can be used after approximately 24 h, when equilibrium has been reached.

5.2. Final water uptake

As for meranti, the average MC of a 1 mm thick slice directly behind the wood surface is determined and plotted against time in Fig. 10 for pine and in Fig. 11 for acetylated pine. Times at which bound and unbound water are not in equilibrium, thus not representing the average MC, are shown by dashed curves. At $t = 0$, the MC is approximately 9% for pine and 5% for acetylated pine, reflecting the initial MC of the samples. Note that the first profile is obtained before water is placed on the sample so for that profile the calibration can be used. The curves are given for the full length of the experiment to show that equilibrium is reached after approximately 20 h. From that moment in time, the solid parts of the curves accurately represent the MC.

A final MC of approximately 48% is observed for uncoated pine and 25% for uncoated acetylated pine. This is in accordance with
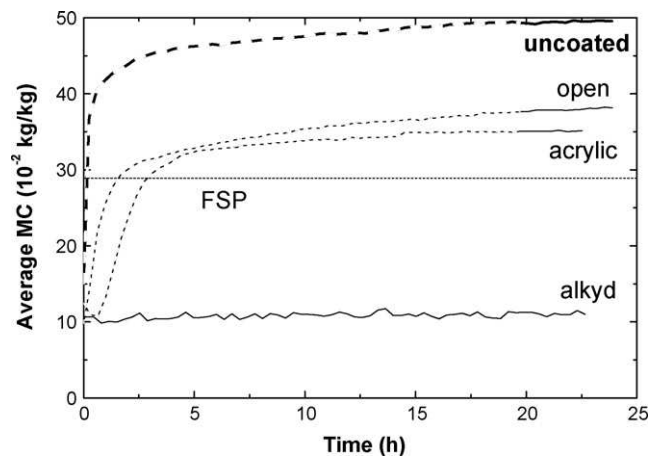

Fig. 10. Average MC of a 1 mm thick slice of pine directly behind the wood–coating interface, plotted against time. Curves are shown for a coating thickness of 100 μm or a mass of 50 g m⁻². The horizontal dashed line indicates the FSP. When the calibration cannot be used, the curves are dashed.
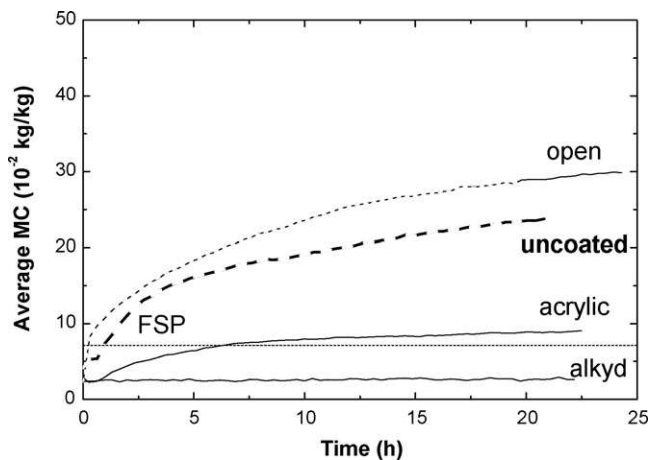
Fig. 11. Average MC of a 1 mm thick slice of acetylated pine directly behind the wood–coating interface, plotted against time. Curves are shown for a coating thickness of 100 μm or a mass of 50 g m^{-2}. The horizontal dashed line indicates the FSP. When the calibration cannot be used, the curves are dashed.

a lowering of the FSP to 7% instead of 29% as a result of acetylation. The alkyd coating on pine and meranti show similar behavior. In both cases moisture absorption was almost fully inhibited. The open coating reduces the uptake of pine, but shows no influence on the uptake of acetylated pine. This is most probably due to incomplete sealing of the rays in the latter case, because the open coating is a non film-forming stain. The observed difference in final MC of uncoated and open coated acetylated pine is caused by an annual ring observed at the top of the uncoated acetylated pine sample. The acrylic coating limits the MC approximately to the FSP, which in the case of acetylated pine is already very low.

5.3. Performance of the coatings

To determine how the coatings reduce the water uptake, a relaxation time analysis is performed to assess the state of the water absorbed by the wood. Relaxation time distributions for coated and uncoated pine at the end of the water uptake are plotted in Fig. 12.

The distributions show that the open coating reduces the unbound water uptake. The acrylic coating completely prevents the uptake of unbound water and further reduces the absorption of bound water. This is a result of the film-forming properties of the acrylic coating that seals the rays, only allowing water vapor to
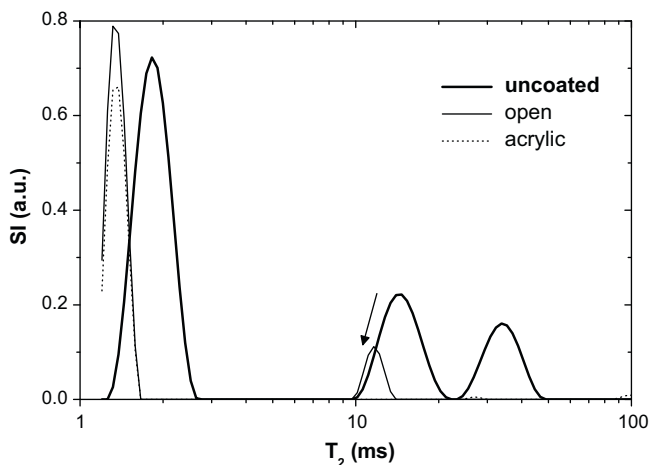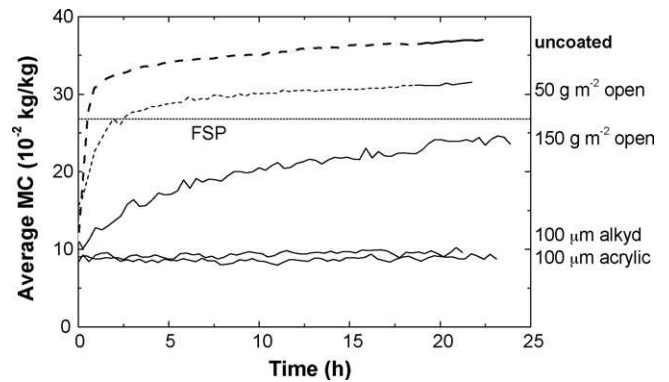

Fig. 13. Average MC of a 1 mm thick slice of spruce directly behind the spruce–coating interface, plotted as a function of time. The horizontal dashed line indicates the FSP. A coating thickness of 100 μm and applied masses of 50 and 150 g m^{-2} are shown.

enter the wood. Similar behavior is observed for acetylated pine. Because the acrylic coating prevents the uptake of unbound water, the calibration can be used throughout the experiment; the corresponding curve in Figs. 10 and 11 is shown solid.

6. Absorption experiments on spruce

Moisture profiles of the water uptake of coated and uncoated spruce were also obtained. The average moisture content of a 1 mm thick slice directly beneath the surface is shown in Fig. 13. Similar to pine, uncoated spruce and 50 g m^{-2} open coated spruce absorb both bound and unbound water at the start of the experiment. As a consequence, the calibration cannot be used. This region is indicated by the dashed sections of the curves.

As with the other types of wood, alkyd coated spruce hardly absorbs any water. The open coating decreases the absorption, depending on the amount of coating applied. The state of absorbed water, bound or unbound, is determined for the uncoated and open coated samples on the basis of relaxation time distributions shown in Fig. 14. The open coating reduces the amount of unbound water uptake. Small contributions at higher relaxation times are present for 50 g m^{-2} open coated spruce, which account for the final MC being above the FSP. 150 g m^{-2} of open coating inhibits the uptake of unbound water and reduces the bound water uptake even more.

The acrylic coating strongly reduces the moisture absorption as shown in Fig. 13, although the acrylic coating absorbs water.
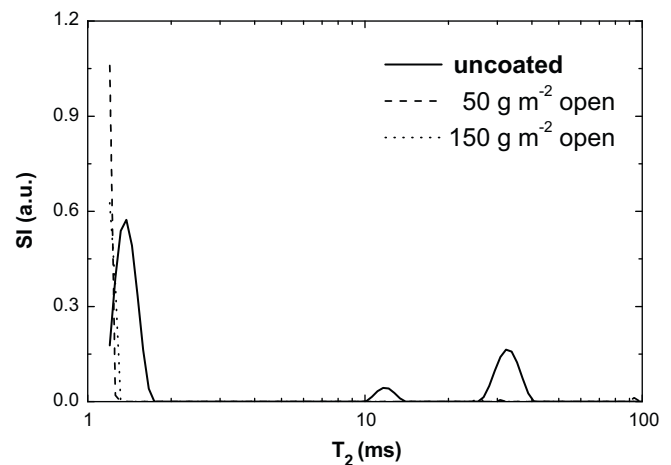

Fig. 12. Relaxation time distributions for coated and uncoated pine after a time of approximately 24 h.

Fig. 14. Relaxation time distributions for uncoated and open coated spruce samples after a time of approximately 24 h.

This behavior largely differs from its behavior on meranti and pine. The reduction in bound water uptake of spruce by the acrylic coating might be a result of wood drying prior to coating application. Because of this, the pits interconnecting the lumina became aspirated. Upon contact with water, the pits reopen, allowing water absorption as seen for uncoated spruce. However, application of the acrylic coating fixates the aspirated pits at the surface of the wood. Despite the absorption of water by the acrylic coating, water no longer flows or condensates in lumina beneath the sealed pits. Moisture can only enter the wood through evaporation from the coating in a pit and subsequent vapor transport through the lumina. This strongly reduces the water uptake.

de Meijer and Militz [10] give another possible cause for the reduction of water uptake. By weighing spruce samples, they found that an acrylic coating strongly reduces the water absorption of spruce. Using micro tomography, they concluded that an acrylic coating penetrates only the first two cell layers of spruce whereas in pine a coating was observed to penetrate much deeper, up to 1000 μm [27]. As suggested previously, fixation of the aspirated pits in spruce may be causing this. Alternatively, de Meijer suggests that, due to the small size of the pits of spruce (2–5 μm, compared to 10–25 μm for those of pine), they are more easily clogged with agglomerates of pigment particles. However, from impregnation studies, the permeability of dried spruce is known to be much lower than that of undried spruce [28,29], largely as a result of the aspiration of bordered pits. Therefore, the low water uptake of acrylic coated spruce is most likely a result of pit aspiration caused by drying of wood. The open coating only fixates part of the aspirated pits. The extent depends on the amount of coating applied, since the open coating contains less binder material.

7. Conclusions

7.1. NMR measurement technique

NMR has proven to be an excellent tool to determine the wood moisture content of coated and uncoated wood samples during water absorption. In contrast to weighing techniques, NMR allows to determine the MC spatially and dynamically. Both the amount and rate of water uptake are determined with high accuracy in relatively short experiments. Additionally, the accuracy is increased with respect to weighing measurements because water does not have to be removed from the sample between subsequent measurements. Also, NMR distinguishes between bound and unbound water, which allows to characterize the state of absorbed water. Because of the fast initial capillary water uptake of pine and spruce, a steady-state calibration as presented in this paper cannot be used at the start of the experiments. At that time bound and unbound water are not yet in equilibrium. However, after approximately 24 h the steady-state MC of all four wood species is reached and can thus be determined accurately.

7.2. Coatings on wood

The influence of the coatings on the water absorption can be summarized as follows. The open coating has no influence on the water absorption, when applied on meranti and pine, because this coating is not a film-forming system. Tripling the applied mass has no influence on the water uptake of meranti. Although the effect of an increased amount of coating mass was not studied for pine, it is expected to have no influence. The open coating reduces the absorption of spruce by clogging a part of the pits near the surface, the extent of which depends on the amount of coating applied.

The alkyd coating inhibits moisture absorption of the woods studied. This coating hardly absorbs any water and seals rays. As a consequence, it forms an effective barrier against moisture.

In case of the acrylic coating, the wood type is of great influence on the moisture absorption. For acrylic coated meranti, the final amount and rate of water uptake are equal to uncoated meranti. Note that only the cell walls absorb water. Therefore, the acrylic coating offers no protection for meranti against water, which is caused by the absorption of relatively large amounts of water by the coating. The coating thickness had no significant effect on the water uptake. On pine, the acrylic coating seals the relatively large rays, thereby reducing the absorption of unbound water by approximately 40–50%. However, as in the case with meranti, the acrylic coating does not prevent water uptake of the cell walls. Because of its low FSP, this resulted in a low final moisture content in case of acetylated pine. In case of spruce, the acrylic coating almost completely inhibits water absorption, by cell walls, lumina and rays. This is most likely the result of fixation of aspirated pits near the surface by coating constituents.

7.3. Concluding remarks

The differences between the behavior of the various wood-coating combinations can be understood as follows. The water absorption of the studied uncoated wood samples is either dominated by diffusion (hardwood meranti) or by capillary uptake (softwoods pine and spruce). In the case of diffusion dominated absorption, the water uptake of the applied coating determines the water uptake of the wood (high/low uptake of acrylic/alkyd coating results in high/low uptake of meranti). In the case of capillary dominated absorption, a film-forming coating (alkyd or acrylic) seals the capillaries (rays and lumina). The absorption is largely determined by diffusion and therefore dependent on the water uptake of the coating.

The water uptake of the studied coating differs largely. Since the acrylic coating is waterborne, it contains surfactants and coalescing agents. These are hydrophilic and contribute to the high water uptake of this coating. Since these additives are known to leach from the coating during outdoor exposure, the water absorption of the coating is reduced in course of time, thereby improving its performance. The solvent borne alkyd coating is prepared from a molecular solution and has a hydrophobic character resulting in low water uptake.

This research has shown that the moisture permeability of a coating dependents on the specific combination of wood and coating. These cannot be treated separately because the coating influences the moisture sorption of wood in different ways. As a consequence, the performance of these coatings should be assessed in a manner suitable for the specific coating.

References

[1] M. Rutte, Wijziging arbeidsomstandighedenregeling, Staatscourant (2004).
[2] J. Hoogervorst, Wijziging arbeidsomstandighedenregeling betreffende werkzaamheden met vluchtige organische stoffen, Staatscourant (2001).
[3] E. Commission, VOC Paints Directive (2004/42/EC), 2004, http://www.ec.europa.eu/environment/air/pollutants/paints_directive.htm.
[4] E. Commission, Registration, evaluation and authorization of chemicals (EC 1907/2006), 2006, http://www.ec.europa.eu/environment/chemicals/reach/reach_intro.htm.
[5] M. de Meijer, Interactions between wood and coatings with low organic solvent content, Ph.D. thesis, University of Wageningen, 1999.

[6] P. Wiberg, S. Sehlstedt-P, T. Morén, Heat and mass transfer during sapwood drying above the fibre saturation point, Drying Technology 18 (2000) 1647–1664.

[7] O. Plumb, G. Spolek, B. Olmstead, Heat and mass transfer in wood during drying, International Journal of Heat and Mass Transfer 28 (1985) 1669–1678.

[8] B. Time, Studies on hygroscopic moisture transport in Norway spruce (*Picea abies*). Part 1: sorption measurements of spruce exposed to cyclic step changes in relative humidity, Holz als Roh- und Werkstoff 60 (2002) 271–276.

[9] B. Time, Studies on hygroscopic moisture transport in Norway spruce (*Picea abies*). Part 2: modelling of transient moisture transport and hysteresis in wood, Holz als Roh- und Werkstoff 60 (2002) 405–410.

[10] M. de Meijer, H. Militz, Moisture transport in coated wood. Part 1: analysis of sorption rates and moisture content profiles in spruce during liquid water uptake, Holz als Roh- und Werkstoff 58 (2000) 354–362.

[11] M. de Meijer, H. Militz, Moisture transport in coated wood. Part 2: influence of coating type, film thickness, wood species, temperature and moisture gradient on kinetics of sorption and dimensional change, Holz als Roh- und Werkstoff 58 (2001) 467–475.

[12] R. Gummerson, C. Hall, W. Hoft, Unsaturated water flow within porous materials observed by NMR imaging, Nature 281 (1979) 56–57.

[13] A. Rosenkilde, J. Gorce, A. Barry, Measurement of moisture content profiles during drying of Scots pine using magnetic resonance imaging, Holzforschung 58 (2004) 138–142.

[14] A. Rosenkilde, P. Glover, High resolution measurement of the surface layer moisture content during drying of wood using a novel magnetic resonance imaging technique, Holzforschung 56 (2002) 312–317.

[15] J. Ekstedt, A. Rosenkilde, S. Hameury, M. Sterley, H. Berglind, Measurement of moisture content profiles in coated and uncoated Scots Pine using Magnetic Resonance Imaging, in: COST E 53 Conference—Quality Control for Wood and Wood Products, 27–32, 2007.

[16] R. Menon, A. MacKay, J. Hailey, M. Bloom, A. Burgess, J. Swanson, An NMR determination of the physiological water distribution in wood during drying, Journal of Applied Polymer Science 33 (1987) 1141–1155.

[17] R. Menon, A. MacKay, S. Flibotte, J. Hailey, Quantitative separation of NMR images of water in wood on the basis of T_2, Journal of Magnetic Resonance 82 (1989) 205–210.

[18] C. Araujo, A. MacKay, J. Hailey, K. Whittall, H. Le, Proton magnetic resonance techniques for characterization of water in wood: application to white spruce, Wood Science and Technology 26 (1992) 101–113.

[19] C. Araujo, A. MacKay, K. Whittall, J. Hailey, A diffusion model for spin–spin relaxation of compartmentalized water in wood, Journal of Magnetic Resonance Series B 101 (1993) 248–261.

[20] Y. Xu, C. Araujo, A. MacKay, K. Whittall, Proton spin-lattice relaxation in wood—T_1 related to local specific gravity using a fast-exchange model, Journal of Magnetic Resonance Series B 64 (1996) 55–64.

[21] G. Almeida, S. Gagné, R. Hernández, A NMR study of water distribution in hardwoods at several equilibrium moisture contents, Wood Science and Technology 41 (2007) 293–307.

[22] J. Siau, Transport Processes in Wood, 1st ed., Springer-Verlag, 1984.

[23] C. Hill, Wood Modification: Chemical, Thermal and Other Processes, John Wiley & Sons, 2006.

[24] E. Hahn, Spin echoes, Physical Review 80 (1950) 580–594.

[25] J. Bear, Y. Bachmat, Introduction to Modeling of Transport Phenomena in Porous Media, 4th ed., Kluwer, Dordrecht, The Netherlands, 1990.

[26] M. de Meijer, H. Militz, Sorption behaviour and dimensional changes of wood–coating composites, Holzforschung 53 (1999) 553–560.

[27] M. de Meijer, Comparative study on penetration characteristics of modern wood coatings, Wood Science and Technology 32 (1998) 347–365.

[28] T. Ulvcrona, H. Lindberg, U. Bergsten, Impregnation of Norway spruce (*Picea abies* L. Karst.) wood by hydrophobic oil and dispersion patterns in different tissues, Forestry 79 (2006) 123–134.

[29] T. Olsson, M. Megnis, J. Varna, H. Lindberg, Study of the transverse liquid flow paths in pine and spruce using scanning electron microscopy, Journal of Wood Science 47 (2001) 282–288.